energies

Review

Performance Augmentation of the Flat Plate Solar Thermal Collector: A Review

Tabish Alam [1,2,*], Nagesh Babu Balam [1,2], Kishor Sitaram Kulkarni [1,2], Md Irfanul Haque Siddiqui [3], Nishant Raj Kapoor [2], Chandan Swaroop Meena [1,2], Ashok Kumar [1,2] and Raffaello Cozzolino [4,*]

[1] Building Energy Efficiency Division, CSIR-Central Building Research Institute, Roorkee 247667, India; nagesh.balam@gmail.com (N.B.B.); kishorsk@cbri.res.in (K.S.K.); chandanswaroop2008@gmail.com (C.S.M.); kumarcbri@rediffmail.com (A.K.)
[2] Academy of Scientific and Innovative Research (AcSIR), Ghaziabad 201002, India; talks.nishant@gmail.com
[3] Mechanical Engineering Department, King Saud University, Riyadh 11421, Saudi Arabia; msiddiqui2.c@ksu.edu.sa
[4] Department of Engineering, University of Rome Niccolò Cusano, 00166 Roma, Italy
* Correspondence: tabish.iitr@gmail.com (T.A.); raffaello.cozzolino@unicusano.it (R.C.)

Abstract: The need for hot water in residential buildings requires a significant energy potential. Therefore, an efficient water heating system is important to achieve the goal of saving high-grade energy. The most simple and cheapest solar water heater is a flat plate solar collector (FPSC), which can increase the thermal energy of fluid by absorbing solar radiation. The performance of FPSC is comparatively low due to the dilute nature of solar insolation. Therefore, advancement of FPSC is being undertaken to improve the performance and achieve size reduction. In past, several techniques have been exploited to improve the performance of FPSC, which are presented in the present paper. These techniques include surface modifications, use of nanofluids, solar selective coating, and applications of a mini/macro channel, heat pipe, and vacuum around absorber. Surface modification on the absorber/absorber tube techniques are exploited to transfer the maximum possible solar energy to working fluids by increasing the heat transfer rate. Insertion of wire mesh, coil, and twisted tapes in the flow has great potential to increase the Nusselt number by 460% at the expense of a large pressure drop. Selective coating of Cu0.44 Ti0.44 Mn0.84 helps to absorb up to 97.4% of the incident solar energy, which is more significant. Many nanofluids have been exploited as heat transfer fluids, as they not only increase the performance but also reduce the fluid inventory. So, these techniques play a very prominent role in the performance of FPSC, which are discussed in detail. Summaries of the results are presented and recommendations proposed.

Keywords: flat plate solar collector; nanofluid; turbulators; solar selective coating; vacuum

Citation: Alam, T.; Balam, N.B.; Kulkarni, K.S.; Siddiqui, M.I.H.; Kapoor, N.R.; Meena, C.S.; Kumar, A.; Cozzolino, R. Performance Augmentation of the Flat Plate Solar Thermal Collector: A Review. *Energies* **2021**, *14*, 6203. https://doi.org/10.3390/en14196203

Academic Editors: Bashir A. Arima and Philippe Leclère

Received: 28 July 2021
Accepted: 24 September 2021
Published: 28 September 2021

1. Introduction

Generally, energy is produced from naturally occurring resources present in the Earth such as coal, crude oil, natural gas, etc. These resources are limited and will be depleted in few years due to their continuous usage. Apart from conventional energy sources, renewable energy sources, such as geothermal, tidal, hydro, and solar energy, are green sources of energy, which can be renewed. Among all renewable energy, solar energy is one of the vastest sources of energy due to its ubiquitous nature, and it is omnipresent and freely available everywhere. Solar energy can be utilized by various thermal systems like solar cookers [1], solar water heaters [2], solar heating [3,4], solar energy harvesting [5] and to produce greenhouse effects [6], solar heat pumps [7], photovoltaic panels [8], and desalination [9], etc. Solar energy can be converted into direct or indirect forms of other energy, such as mechanical, electrical, chemical, etc. The conversion of solar energy into mechanical energy happens in solar thermal plants for power generation. The conversion of solar energy into chemical energy is found in green plants, which takes place by the process of photosynthesis. However, conversion of solar energy into useful energy is considered to occur mainly in two broad ways: (i) solar–thermal conversion by solar thermal collectors, and (ii) solar-electric conversion by using photovoltaic solar cells. The most common solar systems are solar thermal collectors (STCs), which produce the thermal energy of fluids. STCs are classified broadly on the collector design and tracking arrangement as shown in Figure 1. A solar collector may be non-tracking collectors (NTCs) and tracking collectors (TCs). NTCs are fixed and unable to move with the movement of the sun. They include the compound parabolic collector (CPC), evacuated tube collector (ETC), hybrid photovoltaic/thermal collector (PV/T), and flat plate solar collectors (FPSCs). However, TCs are designed to follow the Sun's path, which can absorb maximum insolation. Tracking collectors can also be classified based on single-axis tracking collectors (SATCs) and double-axis tracking collectors (DATCs). Single-axis collectors can move about a single axis, which includes the linear Fresnel collector (LFC), cylindrical trough (CT), and parabolic trough (PT). Double-axis tracking collectors can rotate about two axes that are perpendicular to each other. These two axes can rotate with respect to each other in such a way that the collector may be exposed to track maximum solar radiations. The circular Fresnel lens (CFL), parabolic dish receiver (PDR), and central tower receiver (CTR) are included in this category of DATCs [10]. Different collectors have been used in a variety of applications. FPSCs can supply hot water at moderate temperatures (up to 80 °C), which may be best suited for bathing, washing clothes and utensils, and heating rooms of residential buildings. SATCs, e.g., CPC, PV/T PTC, LFR, can supply fluid thermal energy at a temperature of up to 500 °C, and are used generally in power plants, textile, cement, food, and plastic industries, etc. [11]. Despite this, they can also be operated at temperatures of up to 1500 °C and examples are CTR and PDR [11]. A summary of the different collectors is presented in Table 1. Additionally, the efficiency and working temperatures of different collectors are presented in Figure 2 for ready reference. It is indicated in Table 2 that the efficiency of FPSCs is low compared to other SCs, which is due to high convective heat losses (heat losses through glass cover).

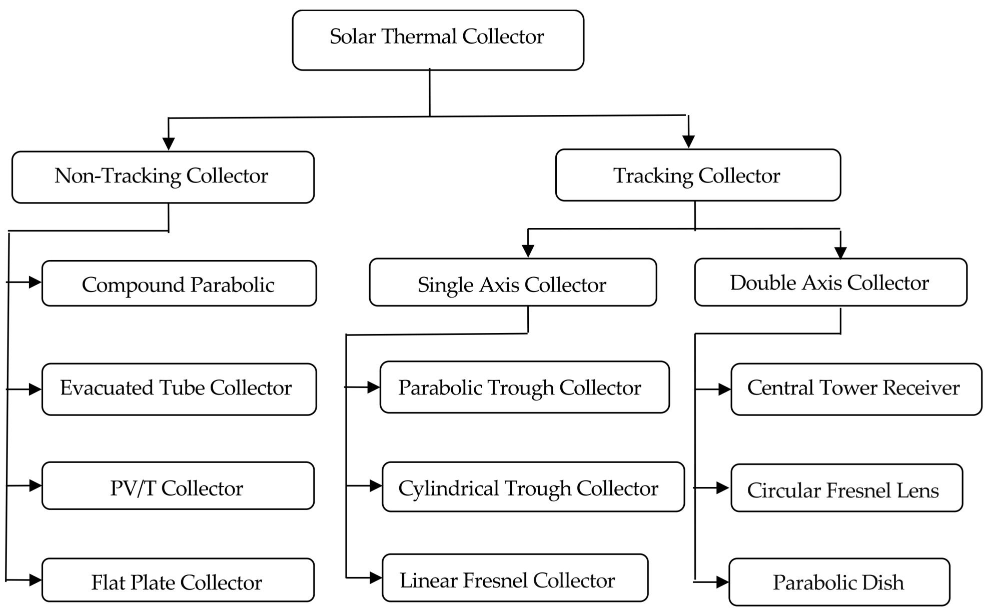

Figure 1. Classification of solar collectors by tracking arrangement [11,12].

Table 1. Detailed summery of solar thermal collectors [11,12].

Collector Typology	Absorber Type	Efficiency (η) in %	Working Temp. (°C)	Applications
Flat Plate Collector	Flat	30–50	Up to 80	Domestic purposes
Evacuated Tube Collector	Flat	30–50	Up to 200	Domestic purposes, Heating/cooling of space,
Compound Parabolic	Tubular	~60	110–200	Domestic purposes, Heating/cooling of space,
PV/T Collector	Tubular	Up to 50	Up to 60	Domestic purposes, Heating process.
Parabolic Trough Collector	Tubular	50–70	150–500	Heating/cooling of space, Power plant, Textiles industry
Cylindrical Trough Collector	Tubular	Up to 50	Up to 400	Domestic purpose, Heat process, Power plant
Linear Fresnel Receiver	Tubular	Up to 50	Up to 500	Steam generation, Heat process, Power plant
Central Tower Receiver	Point	40–65	Up to 1000	Power generation, Heat process
Parabolic Dish Receiver	Point	60–75	Up to 1500	Power generation, Heat process

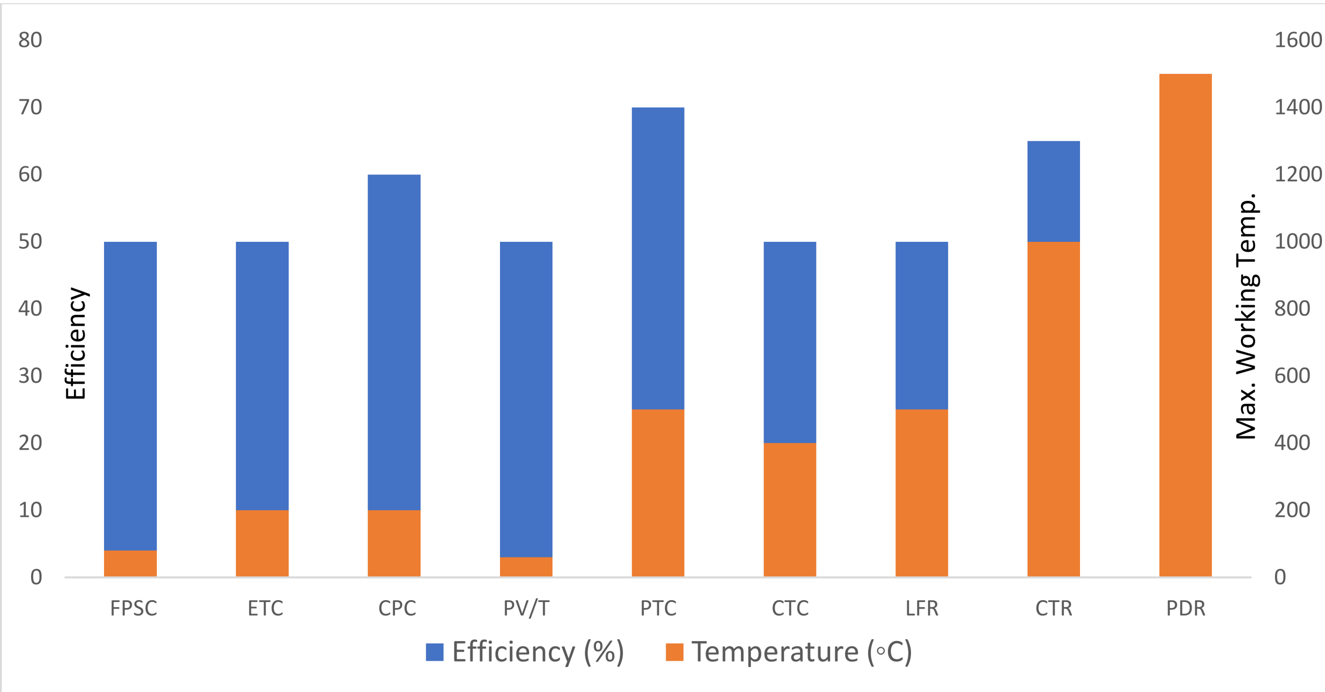

Figure 2. Efficiency and working temperatures of various STCs [11,12].

A lot of studies have been reported in the literature. A few highlighted the study on solar thermal collectors. Kalogirou [12] presented reviews of various solar thermal collectors with their merits and demerits. The performance based on optical and thermal analysis of the various collectors was presented. Suman et al. [11] presented an extensive review on advancements in solar thermal technology and discussed the various factors involved in performance augmentations. Said et al. [13,14] summarized and discussed the most important studies based on nanofluid that are exploited in solar systems for applications at low and medium temperatures. Jabrej et al. [15] presented an overview of energy analysis, exergy analysis, heat transfer analysis, performance analysis, and transient analysis of various solar flat plate collectors. Although, there is still scope to present a review on the FPSCs and techniques that have been exploited to improve their performance.

Therefore, the objective of this paper is to review the various performance improvement techniques exploited in FPSCs with an emphasis on employing these techniques efficiently. It also covers the description of different techniques that have facilitated the systematic understanding and the novel modifications realized to obtain an efficient and compact design of FPSCs.

2. Methodology Adopted for Review

The literature review is an important foundation to serve as knowledge development, to explore the research gaps, create guidelines for policy, and provide evidence. Additionally, the literature review serves as a base for future research. This paper presents a literature review of different techniques used to enhance the performance of flat plate solar thermal collectors. Several efforts have been made to collect the information on techniques that have been presented here. In order to gather as much information on the techniques used in FPSCs, relevant scientific articles were searched with the following keywords: solar collector, flat plate solar thermal collector, performance, artificial roughness, geometrical modification, heat transfer fluids, nanofluid, heat pipes, solar coating, etc. The information from the various download papers was summarized and categorized based on the performance improvement techniques.

3. Flat Plate Solar Collector (FPSC)

The FPSC is a type of heat exchanger, and the basic function of FPSC is to convert solar energy into thermal energy of fluids. Typically, FPSCs have four main components, namely a transparent glass cover, absorber plate, fluid passage, and housing. The top glass covers are used to reduce the top heat losses by minimizing natural convection. Double or multi glass covers can reduce the top heat losses significantly at the penalty of reduced transmissivity of radiation. Three sides (back and both sides) of the collector are covered with insulation covers. Metallic tubes are attached beneath the absorber plate for heat transfer fluids (e.g., water, oil, etc.). Proper insulating materials are placed on metallic tubes and the bottom wall of the collector enclosure. FPSC is usually fixed to face the south in the northern hemisphere and the north direction in the southern hemisphere. A schematic diagram of a typical FPSC is shown in Figure 3.

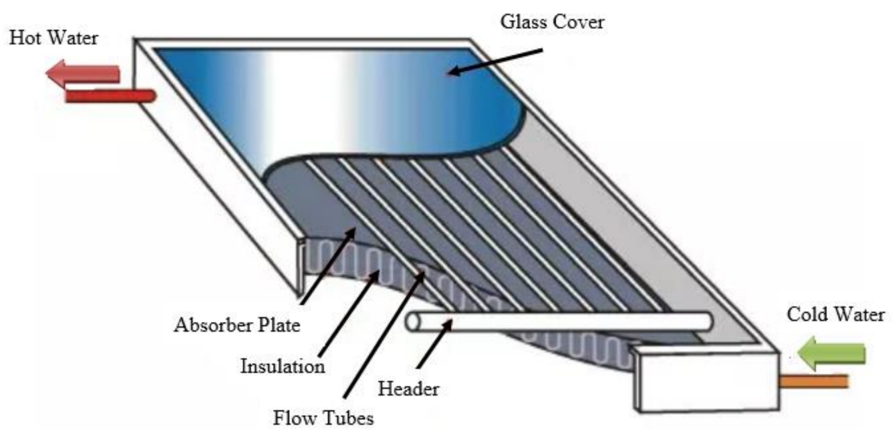

Figure 3. Typical FPSC [16].

A typical FPSC is designed to supply water at moderate temperatures (up to 80 °C) for domestic purposes. FPSCs are mechanically simpler than other collectors. FPSCs can absorb diffuse radiation in addition to direct radiation, which is the main advantage. The system requires little or no maintenance except cleaning of the glass cover. Initially, the performance of FPSCs has been low due to high heat loss, low absorptivity, low convection heat transfer coefficient, etc. [10]. In this regard, researchers have attempted to develop new techniques for designing efficient FPSCs. The aim of this manuscript is to review the research progress in the performance improvement of FPSCs. Further, the effect of parameters and the key results of selective studies are presented and discussed.

4. Advancement in FPSCs

Some recent methodology/techniques have been implemented with an aim to increase the overall performance. High thermal efficiency, low cost, and reliable operation under extreme weather conditions are the basic requirements of a perfect FPSC. In this regard, researchers have developed and explored techniques that help to develop efficient collectors. These techniques include modifications of the geometries in the absorber tube and/or collector, use of nanofluids, solar selective coating on the absorber, use of heat pipes, mini/macro channels for heat transfer fluids, and heat loss reduction. Figure 4 presents the different performance improvement techniques, and the advancement of these techniques is discussed in subsequent sub-sections.

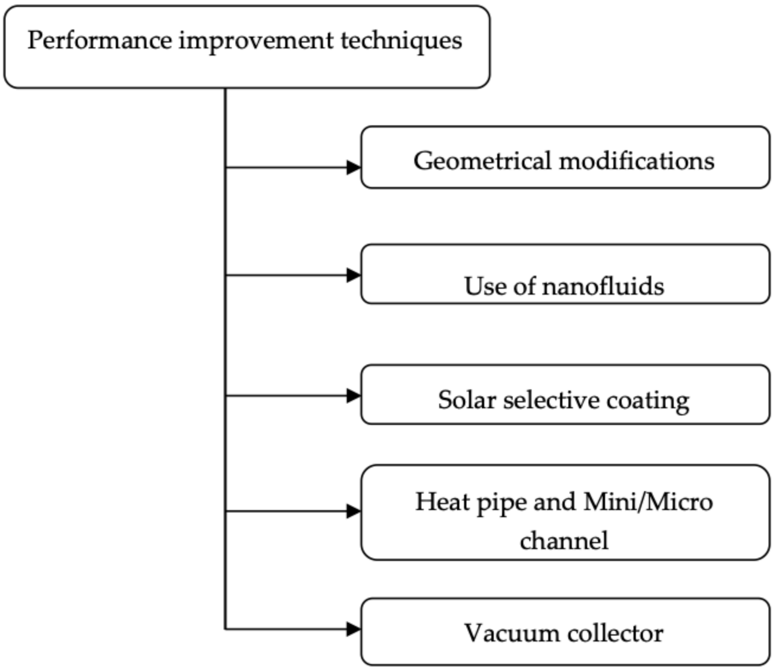

Figure 4. Performance improvement techniques of FPSCs.

4.1. Geometry Modification

Generally, the heat transfer capability of the smooth surface from the absorber plate/tube is low due to the low convective heat transfer coefficient, which causes poor performance. Heat transfer can be enhanced by increasing the heat transfer areas (i.e., fins) and creating turbulence, which tends to break the laminar-sub layer and mix different fluid layers. Corrugations/fins/extended surfaces in absorber tubes are exploited for heat transfer enhancement. Surface modification in the receiver tends to increase the pressure drop penalty and hence, increases the consumption of pumping power [11]. Therefore, it becomes necessary to design surface roughness that provides the maximum heat transfer coefficient with the minimum pressure drop [17]. Various geometrical shapes have thus been tested for the absorber and/or tube of collectors. In this regard, Hobbi and Siddiqui [18] studied the effect of turbulators in FPSCs, namely a coil-spring, conical ridges, and twisted strip. Mwesigye et al. [19] studied the effect of perforated plates placed in receiver tubes to reduce the temperature gradient. As a result of the perforated plate inserts, the temperature gradient of the receiver decreased significantly, and the thermal efficiencies of the collector increased up to 8%.

Sahin et al. [20] presented a concentric heat exchanger tube equipped with coiled wire turbulators as the receiver of the collector. A maximum heat transfer enhancement od 2.28 times with respect to the smooth tube was reported. Fuqiang et al. [21,22] introduced an asymmetric/symmetric tube with an outward convex corrugated in the parabolic trough. It was concluded that the overall heat transfer performance factors were enhanced by 26.8% and 148%, respectively. Song et al. [23] numerically studied the effect of helical screw tape inserted in the absorber tube to homogenize the temperature distribution. As a result of the helical screw inserts, the heat losses and temperature gradient were reduced, which indicated that the technique was feasible for performance improvement. Wang et al. [24] numerically explored the performance of a receiver tube filled with metal foam. The effect of the porosity, geometrical parameters, and layout (top/bottom) of the metal foam on heat transfer and flow resistance have been investigated. Optimum thermal performance was obtained when a Nusselt number and friction factor ratio 10–12 times and 400–700 times with respect to that without metal foam, respectively, were achieved. Four different enhanced receiver tube (ERT) configurations, namely (a) cylinder-shaped porous insert filled in the core of the receiver tube (ERT-I), (b) hollow cylinder-shaped porous insert attached to the inner surface of the receiver tube (ERT-II), (c) horizontal cylindrical segment-shaped porous insert filled in the lower part of the receiver tube (ERT-III), and (d) horizontal cylindrical segment-shaped porous insert filled in the upper part of the receiver tube (ERT-IV), were modelled to optimize the performance, carried out by Zheng et al. [25]. It was recommended that ERT-II and ERT-IV exhibited good thermo-hydraulic performance to obtain a high conductivity ratio and ERT-II could be exploited in the best way at low porosity.

The effect of wire-coil inserts in tube-on-sheet solar collectors was explored using the TRNSYS simulating tool [26]. The friction factor, local losses, and Nusselt number were evaluated for standard collectors under the same radiant, ambient, and operating conditions. It was reported that the efficiency was increased by 4.5%. Axtmann et al. [27] investigated the effect of pin-fin arrays having pin-fins along with long and short elements. Three configurations, with an aspect ratio $2 \leq H/D \leq 5$ and a relative spacing $2.5 \leq S/D \leq 5$, were tested using the transient liquid crystal technique. Pin-fin arrays inserts decreased the thermal boundary layer, leading to a comparatively higher heat transfer rate. Chin et al. [28] performed experimental and numerical investigations on staggered pin fins in an absorber tube. Increases in the Nusselt number of 45% for the perforated pins and the pressure drop of 18% for solid pin fins of a similar size were reported. Gong et al. [29] carried out a study on the overall performance enhancement of an absorber tube using pin fin arrays. The authors reported that this novel technique could effectively enhance the Nusselt number and overall performance by up to 9.0% and 12.0%, respectively.

Reddy [30] experimentally tested a solar collector with different porous disc receivers in an absorber tube. Performances were evaluated in terms of daily performance, peak performance, collector acceptable angle, time constant, and heat loss tests. It was reported that efficiencies in the range of 63.99–66.66% could be achieved. Under fully developed turbulent flow, three different roughness, namely dimple, protrusions, and helical fins, on receiver walls were investigated numerically [31]. The dimple ribs exhibited a better performance in compared to the other ribs investigated. Additionally, dimples with a narrow pitch, deeper depth, and more numbers in the circumference were found to be better amongst all arrangements. Jamal-Abad et al. [32] investigated the performance of an absorber tube filled with metal foam in the collector. The metal pore density and porosity were considered as 30 PPI and 0.9, respectively, and the volume flow rate was employed in the range of 0.5 to 1.5 L/m. The overall heat loss coefficient was reduced by 45%, which led to an improvement in the receiver efficiency.

Most researchers have reported that the use of a metal pipe as an absorber is a suitable technique to increase thermal performance. Although, these collectors are heavy, non-versatile, and have a complex design, and have shown high hydraulic resistance along with low thermal performances. In order to eliminate these difficulties, Rassamkin et al. [33]

used an extruded aluminum pipe with longitudinal grooves and long fins as an absorber. Fins on the opposite side of the heat pipe served as a heat sink. The proposed heat pipe configuration was found to be thermally and hydraulically efficient. Sandhu et al. [34] conducted an experimental study of different insertion devices and the influence of inclination on the collector efficiency. The results showed that concentric coils were recommended as the best insert device due to a higher enhancement of the Nusselt number, reported as 460% and 110% in a turbulent and laminar flow regime, respectively. Garcia et al. [35] investigated the effect of three wire-coils and three twisted-tapes in an absorber tube. It was reported that wire coil with a moderate pitch to diameter ratio exhibited the best performance among all the inserts. Balaji et al. [36] explored the effect of two different heat transfer enhancers, namely rod and tube heat transfer enhancers, in the riser tube of FPSC. It was reported that minimum and maximum exergy efficiency was found for rod and tube heat transfer enhancers, respectively. Anirudh and Dhinakara [37,38] studied the performance of FPSC in which porous metal foam blocks were utilized to promote thermal mixing. These blocks were arranged in different ways on the absorber plate. The effects of the permeability of the porous medium and height of the porous block on the collector outlet temperature were studied. The increment was prominent for higher values of the height of porous blocks due to improved thermal mixing. The thermal performance of FPSC exploiting V-corrugated absorbers was studied in detail [39]. The transfer function model (TFM), dynamic heat transfer model (DHTM), and quasi-dynamic test model (QDTM) were implemented to predict the performance. It was indicated that DHTM could accurately predict short-term thermal performance. Gao et al. [40] exploited a novel glazed transpired collector system with non-uniform perforation. The thermal characteristics, namely the temperature rise, heat exchange efficiency, heat collection efficiency, and collector heat loss coefficient, were analyzed under different operating conditions. The results indicated that the efficiency and temperature were 20% and 6 °C higher, respectively, with respect to traditional FPSC. Important investigations are summarized in Table 2 for ready reference.

Table 2. Selective study on the surface modification of the absorber tube.

Authors	Modification of Surface	Study Type	Ranges of Parameters	Test Fluids	Key Results
Mwesigye et al. [19]	Centrally placed perforated plate inserts	Numerical	Re = $1.02 \times 10^4 - 7.38 \times 10^4$, m = 47.7 − 56.3 L/min, p = 0.08–0.20, d = 0.45–0.61	Water	Increment in efficiency by 1.2–8%
Sahin et al. [20]	Coil wire turbulators	Numerical and Experimental	Re = 3000–17,000, p = 15–60 mm	Water	Heat transfer increased by was 2.28 times.
Fuqiang et al. [21,22]	Outward corrugated convex tube	Numerical	For CPTR, p/D (CPTR) = 4.3–14, Re = 18,860–81,728 For ACPTR p/D = 1.11–7.25, Re = 8600–81,784	Water	Performance factor enhanced by 148%.
Song et al. [23]	Helical screw tape inserts	Numerical	–	water	Heat losses decreased by 6 times w.r.t. to smooth tube.
Wang et al. [24]	Metal foam inserts	Numerical Simulation	h/Di = 0–1, ϕ = 0.9132–0.9726, PPI = 5–40 Re = 1064–894,000	Water/Steam	Nusselt increased in the range of 5–10 times.
Zheng et al. [25]	Porous material inserts	Numerical simulation	ϕ = 0.9726–0.9546, PPI = 5–40, Re = 30,000–90,000	Mixed nitrate molten salt	Thermal conductivity ratio should be more than 100 for better performance.
Axtmann et al. [27]	Staggered arrays of adiabatic pin fins	Experimental	S/D = 2.5–5, H/D = 2–4, Re = 3000–30,000	Air	Large pin fin spacing provides better hydraulic efficiency
Chin et al. [28]	Staggered perforated fin pins	Experimental and numerical both	No of holes (N) = 0–5, Hole dia (D_p) = 0–4 mm,	Air	Nusselt number increased by 45%.
Gong et al. [29]	Pin fin array	Numerical simulation	m = 0.51–0.73 kg/s	D12 Thermal oil	Heat transfer performance increased by 12.0%

Table 2. *Cont.*

Authors	Modification of Surface	Study Type	Ranges of Parameters	Test Fluids	Key Results
Reddy et al. [30]	Porous Disc	Experimental	m = 100–1000 L/h DNI = 500–900 W/m^2,	Water	Range of efficiencies reported from 63.9 to 66.66%.
Sandhu et al. [34]	wire mesh insert, wire coil, and twisted tapes	Experimental	Re = 200–8000	Water	Nusselt number increased by 460%.

4.2. Solar Selective Coating

Coating on the absorber surface helps to absorb maximum solar energy. Coatings are broadly classified into two different groups: (i) non-selective coating and (ii) solar selective coating. An ordinary black painted surface is a common example of non-selective coating. The solar selective coating has different absorptivity and emissivity for different wavelengths because its optical properties are dependent on solar spectral regions. The basic need of selective coating on the absorber is to increase the absorptivity with minimum emissivity, so that maximum energy can be retained. The solar selective coating should have high selectivity for the best performance. Shaffer [41] proposed an application of selective coating on the solar collector surface. Since then, different varieties of selective coating have been developed, which was summarized by Chen [42]. Although, solar selective coatings are very expensive and require special treatment of the absorber.

Generally, solar selective coatings have low emissivity in the long-wave spectral range (i.e., more than 2.5 μm). The selective coating absorbs incoming radiation and helps to minimize the emission of longer wavelength radiation. Therefore, selective solar coating helps to absorb solar irradiation and maintains the surface at a high temperature [43]. Various studies have developed more efficient solar selective coatings for the best performance and to trap maximum solar insolation, such as semiconductor-metallic layers, particulate coating, multi-layer films, etc. Cindrella [44] studied the performance of composite selective black coating of nickel-cadmium and cobalt cadmium on the absorber. It was reported that the developed solar selective absorber coating could be used in a system having a concentration ratio of 1. Tulchinsky et al. [45] presented a method for preparing a novel coating on the copper absorber. This novel thermal coating had absorptivity of 97.4% and 94.7% at 650 and 750 °C, respectively. Abbas [46] experimentally tested metal-based coating, i.e., solchrome selective coating, on three different types of collectors, namely solchrome omega soldered tube with fins collector and solchrome tig welded fin with a tube. It was reported that solchrome coatings could enhance the collector's efficiency in comparison to the ordinary black paint coating. Schuler et al. [47] developed selective coating by incorporation of silicon into titanium-containing amorphous hydrogenated carbon films (a-C:H/Ti). A pump was used to deposit a-C:H/Ti in combination with a liquid nitrogen cooling trap. The experimental results were found to be very promising, i.e., low thermal emittance (0.061) and high absorptivity (0.876). The novel coating is best suited for a vacuum collector as recommended.

Teixeira et al. [48] produced a multi-layered cermet. This composite layered coating was found to be very attractive for photo thermal conversion applications due to its thermal stability. Farooq and Hutchins [49,50] described the development of a multilayer metal-dielectric graded index solar selective coating. The authors reported that four layers of V: Al_2O coating exhibited the best results and showed emissivity of 0.02 and absorptivity of 0.98. Shashikala et al. [51] analyzed a coating of black nickel-cobalt on a pre-cleaned substrate with nickel undercoat. It was reported that the selective coating had favorable optical properties, i.e., high absorptance of 0.948. Additionally, the performance of selective coating has been found to be environment friendly and can be used in space applications. Wazwaz [52] investigated the effects of nickel content in the aluminum layer of selective coating on an absorber. The thermal performance of the absorber was enhanced due to an increase in the nickel content. Beyond a certain value of nickel, i.e., 60 μg/cm^2, the efficiency began to decrease due to an increase in emissivity as reported.

Juang et al. [53] proposed a method to prepare solar selective coating by radio frequency magnetron reactive sputtering using a single stainless steel target. A thermal emittance of 0.91 and absorptance of 0.06 were reported at 82 °C, which was best suited for photothermal conversion applications. Du et al. [54,55] developed a selective coating in which the absorber layer was considered as $Ti_{0.25}Al_{0.75}N$ and $Ti_{0.5}Al_{0.5}N$, whereas the anti-reflective layer was considered as AIN coating. Absorbance and low emittance were reported as 0.945 and 0.04 at 82 °C, respectively.

Nuru et al. [56,57] developed multilayer selective coating of AlxOy/Pt/AlxOy on copper, silicon, and glass. An experimental evaporation system was developed to deposit Pt disc (purity 99.9%) (35 mm in diameter) and Al_2O_3 pellets (purity 99.999%) (3 mm in diameter) on copper crucible. The emittance and absorptance of the optimized multilayer coating were found to be 0.06 ± 0.01 and 0.94 ± 0.01, respectively, at 82 °C. AlxOy/Pt/AlxOy multi-layer coating on a Cu substrate showed significant selectivity (α/ε) of 0.951/0.09 and the coating was thermally stable below 500 °C. Khamlich et al. [58] developed a coating of chromium/α-chromium (III) oxide on a tantalum substrate in a hydrogen atmosphere. High absorptivity has been reported in the temperature range of 400–500 °C. Kumar et al. [59] prepared solar selective coating of copper oxide on a copper substrate by means of copper oxidation at different alkaline conditions. A thin film of CuO covered the whole region of the Cu substrate at different pH. It was found that the emittance and absorptance of these nanostructures of the copper oxide layer were in the range of 6–7% and 84–90%, respectively.

Liu et al. [60] developed a selective coating of four layers. Three layers were made with Cr-Al-O with low, middle, and high oxygen contents and a fourth layer was made of pure chromium. The thermal stability of the coating was found to be good with selectivity of 0.919/0.225. Another nitride-based multi-layered selective coating was developed on an SS absorber with copper substrate using the vapor deposition technique [61]. An appropriate thickness of the different layers in a systematic manner yielded a low emittance of 0.07 and high absorptivity of 0.91, which was attributed to the attractive solar selectivity of 13. Cespedes et al. [62] investigated selective coating, which was developed based on Mo-Si_3N_4. The coating exhibited a high photo conversion efficiency due to precise control of the composition and layer thickness and yielded a low emittance of 0.017 and high solar absorptivity of 0.926. Tsi et al. [63] developed a multilayer coating of CrN(H)/CrN(L)/CrON/Al_2O_3 deposited on stainless steel. The coating layers were designed in such a way that the refractive index increased gradually from the top to the base layer. The values of thermal absorptance and emittance were reported as 0.93 and 0.14, respectively. The results of the various selective coatings are summarized in Table 3 for ready reference.

Table 3. Selective studies on coatings.

Authors	Coating	Surface Material	Optical Properties		Key Results
			ε	α	
Cindrella [44]	Co-Cd-BT Co-Cd-BA Ni-Cd-BT Ni-Cd Co-Cd NI-Cd-BA	Nickel-plated copper	0.12 0.06 0.17 0.10 0.07 0.11	0.96 0.96 0.95 0.94 0.93 0.91	Performance of Ni–Cd–BT coating is high throughout the range considered (100–250 °C)
Tulchinsky et al. [45]	$Cu_{0.44}Ti_{0.44}Mn_{0.84}$- $Fe_{0.28}O_3$	–	0.64	0.97 0.94	solar absorption ranging from 0.88 to 0.94
Abbas [46]	Black chrome	Nickel plated copper	0.12	0.96	Collector was 30% more efficient and coating stable at high temp.
Schuler et al. [47]	a-C:H/Ti	Aluminum	0.061	0.876	the lifetime stability at 250 °C in air could be strongly enhanced.
Teixeira et al. [48]	Cr–Cr_2O_3/Mo–Al_2O_3	Glass, Aluminum and Copper	0.15– 0.04	0.88–0.94	Solar absorption (0.88 to 0.94) is achieved

Table 3. *Cont.*

Authors	Coating	Surface Material	Optical Properties		Key Results
			ε	α	
Farooq and Hutchins [50,51]	$V{:}Al_2O_3$	Copper, aluminum	0.02	0.98,	Solar absorptance of 0.98 and 0.96 was achieved
Shashikala et al. [51]	Black Ni–Co	Nickel-plated aluminum alloy	0.17	0.948	solar absorptance of 0.948 was achieved
Wazwaz [52]	Ni	Aluminum alloy	0.052	0.892	average absorptivity increased by a factor of 4.99–5.35.
Jaung et al. [53]	stainless steel nitride/Stainless steel	stainless steel	0.06	0.91	Solar absorptance of 0.92 was achieved
Du et al. [54,55]	$Ti_{0.5}Al_{0.5}N/Ti_{0.25}Al_{0.75}/AlN$ $Al/Ti_{0.5}Al_{0.5}N/Ti_{0.25}Al_{0.75}N/AlN$	Silicon	0.04 0.04–0.06	0.945 0.926–0.945	absorptance of 0.926–0.945
Nuru et al. [56,57]	AlxOy/Pt/AlxOy	Copper, Silicon, Glass,	0.01	0.94	good spectral selectivity (α/ε) of 0.951/0.09
Khamlich et al. [58]	$Cr/\alpha\text{-}Cr_2O_3$	Tantalum	0.28	0.90	Annealing temperature affected optical properties
Kumar et al. [59]	CuO nanoparticles	Copper	0.06	0.84	Solar absorptances in ranged 84-90% was achieved
Valleti et al. [61]	TiAlCrN/TiAlN/AlSiN	Copper and stainless steel	0.07	0.91	selectivity of 0.919/0.225
Liu et al. [60]	Cr–Al–O	Stainless steel	0.21	0.924	Suitable for collector high temperature
Cespedes et al. [62]	$Mo\text{–}Si_3N_4$	Silicon and stainless steel	0.017	0.926	solar absorptivity of 0.926 was achieved
Tsi et al. [63]	$CrN(L)/CrON/Al_2O_3/CrN(H)/$	stainless steel	0.14	0.93	The coating was thermally stable up to temperatures of 400 °C
Schhular et al. [64]	a-C:H/Ti multilayers	Aluminum	0.061	0.876	14.4 optical selectivity was achieved
Li et al. [65]	$MgO\text{-}ZrO_2$	AZ31 magnesium alloy	0.881 0.914 0.852	0.392 0.375 0.342	Suitable for space craft

4.3. Use of Nanofluid

Generally, heat is extracted from the absorber by means of heat transferring fluids that should possess desirable heat transfer characteristics. Initially, water was known to be a good conductor of heat and was used as the heat transfer fluid in STCs. In recent years, new working fluids have been developed and have shown good potential in thermal conductivity. Srivastava et al. [66] presented a review on heat transfer fluids that are being used in STCs. Working fluids are categorized based on the temperature range of STCs, i.e., high-temperature working fluids, medium temperature, and low temperature. Generally, low-temperature fluids are refrigerants, water, water/glycol mixtures, and nanofluids that are being used in FPSC. Thermic, hydrocarbon oils and some nanofluids come in the category of medium-temperature fluids and molten salt, molten metal, synthetic oil, and inorganic oils come in the category of high-temperature fluids.

In low-temperature fluids, the most common fluids are chlorofluorocarbon (CFC) refrigerants, which are being replaced by hydrochlorofluorocarbons (HCFCs) due to ozone layer depletion. Water is the most commonly used fluid that is being used in FPSC due to its abundant availability, non-toxic nature, free cost, and higher heat capacity; however, it is not favorable in extreme weather conditions. Mixtures of glycol/water are used in a cold climate and these fluids are known as "anti-freezing fluids". The effect of propylene glycol/water mixture in FPSC has shown significant results and the maximum energy output is obtained at 50% concentrations of propylene glycol in water [67].

Nanofluids represent a better option than refrigerants, water, and water/glycol mixtures in FPSC. The thermal conductivity of nanofluids can be altered and desirable properties can be achieved as per the requirements. Several researchers have attempted to enhance the thermal conductivity of HTF by adding nano-sized particles of high thermal conductivity, such as metal, carbon alumina, etc. With the advancement of nanotechnology, new fluids have been prepared by suspended nano-sized particles in base fluids, which are known as nanofluids. Researchers have attempted to enhance the thermal conductivity of nanofluids. Although, aggregation and sedimentation of nanoparticles are major issues that can be resolved by various techniques, such as altering the fluid properties and modifying the collector channel.

Xuan and Li [68] prepared nanofluid by direct mixing of nano phase powders and base fluids. Conductivity was increased with an increase of the copper nanoparticles in water, which varied from 1.24 to 1.78 times that of base fluid alone when the volume fraction of the nanoparticles varied from 2.5% to 7.5%. Colangelo et al. [69] developed diathermic nanofluids with nanoparticles of AlO, CuO, and ZnO. The behavior of the volume fraction of particles (0.0–3.0%) and the shapes of particles on thermal conductivity were investigated. It was shown that diathermic oil with nanoparticles enhanced the heat transfer more than water with the same nanoparticles. The behavior of MWCNT nanofluid was experimentally investigated on the performance of FPSC [70]. As per the ASHRAE standard, tests were performed at different weight fractions and mass flow rates. Substantial efficiency was found with an increase in the weight fraction of nanoparticles as reported. Further, Yousefi et al. [71] utilized Al_2O_3–water nanofluid in FPSC. Nanoparticles of 15 nm were suspended in base fluid in the range of 0.2–0.4% (by wt.) with a volume flow rate of 1–3 L/m. It was reported that the efficiency (η) was increased up to 28.3%. The friction factor and heat transfer characteristics of nanofluids in an absorber tube in turbulent flow conditions were studied by Heyhat et al. [72]. Nanofluid was developed using Al_2O_3 nanoparticles with 40 nm suspended in distilled water. The results showed that the absorber efficiency was increased with an increase in the particle concentration.

Chaji et al. [73] experimentally tested the effect of different nanoparticles of TiO_2 with water as the base fluid in small FPSC. The effects of different particle concentrations (0–0.3% by wt.) and mass flow rates (36–72 l/h) were investigated as per EUROPEAN STANDARD EN 12975-2. An improvement of the initial efficiency of FPSC and index of collector efficiency were reported in the range of 3.5–10.5% and 2.6–7%, respectively. Alim et al. [74] theoretically studied the behavior of various nanofluids (i.e., nanoparticles TiO_2, SiO_2, CuO, Al_2O_3, dispersed in water) inside an absorber tube. It was concluded that the heat transfer coefficient was increased by 22.15%. Moghadam et al. [75] experimentally investigated the effect of CuO-based nanofluid on the efficiency and performance of FPSC. The concentration of nanoparticles and the nanoparticle size were fixed at 0.4% by vol. and 40 nm, respectively. It was reported that an optimum mass flow rate exists for a particular nanofluid.

The heat transfer characteristics of different nanofluids (water-CuO nanofluid, water-Al_2O_3, nanofluid, water-Cu nanofluid, and water-Ag nanofluid) through FPSC were investigated numerically by Nasrin et al. [76]. As per the results obtained, water-Ag nanofluid with a higher volume fraction exhibited the best performance. The effects of Cu nanoparticles on FPSC efficiency were investigated by Zamzamian et al. [77]. The average diameter of nanoparticles was 10 nm and the particle concentration in nanofluid was kept at 0.2% and 0.3% by weight. Due to the higher weight fraction of the nanoparticles, the collector efficiency was increased. The behavior of pH Al_2O_3–H_2O and CuO-H_2O and the performance of a cylindrical solar collector were investigated by Goudarzi et al. [78]. A particle concentration of 0.2% of Al_2O_3 and 0.1% of CuO with various pH values (4.0, 9.2, and 10.5) were exploited to increase the performance of the collector. CuO-H_2O nanofluid with pH = 3 exhibited a collector efficiency improvement of 52%.

Tomy et al. [79] theoretically studied the performance of FPSC, where silver/water nanofluids were used as the heat transfer fluid. The effect of the inlet temperature of the nanofluid along with the operating parameters, i.e., insolations (900–1000 W/m^2) and Reynolds number (5000–25,000), were investigated on the performance of FPSC. The maximum efficiency was reported as 80% at a particular volume fraction of 0.04% of the nanofluid. He et al. [80] studied the behavior of Cu-H_2O nanofluid in FPSC. The experiments were conducted for concentrations of nanofluids 0.1% and 0.2% (by wt.).

Additionally, it was concluded that the performance was improved by 23.83% using nanofluids. It was also reported that the heat gain and temperature were enhanced by up to 24.52% and 12.24%, respectively. Salavati et al. [81] experimentally tested FPSC with SiO_2/ethylene glycol-water nanofluid. The results showed that the efficiency was increased from 4% to 8% with an increase in the particle concentrations from 0% to 1%. Said et al. [82] experimentally tested Al_2O_3-water nanofluid to increase the performance in FPSC. It was reported that the exergy and energy efficiencies increased by 20.3% and 83.5%, respectively.

Direct use of nanofluids in FPSC is a problematic issue, such as nanoparticles aggregation and sedimentation. To overcome these problems, the sedimentation of fluid in both a standard FPSC and modified ones, fabricated from a transparent tube, was studied by Colangelo et al. [83]. He designed the channel in such a way that the fluid axial velocity was fixed. Further, Colangelo et al. [84] explored the behavior of distilled water and Al_2O_3-distilled water-based nanofluid in a modified FPSC. The modified FPSC was designed in such a way to minimize the sedimentation of clusters of nanoparticles. The performance of the FPSC was explored using of Al_2O_3/water-based nanofluid [85]. The mean volume fraction and partial size of nanofluid were considered as 0.1% and 20 nm. It was reported that the optimum collector efficiency was increased up to 23.6% at a 2 L/min mass flow rate. Kilic et al. [86] studied behavior of TiO_2/water nanofluid (2% wt.) to improve the performance of FPSC. It was reported that a 48.67% and 36.20% instantaneous efficiency of FPSC was found for TiO_2/water nanofluid and pure water, respectively.

The effect of different nanoparticle concentrations of magnesium oxide in ethyl glycol (base fluid) was investigated by Harrison et al. [87]. The particle concentrations varied in the range of 0.08–0.2% under varying flow rate conditions. The results indicated that heat gain in FPSC was increased by 16.74% due to a decrease in heat loss of 52.2%. Hussein et al. [80] exploited hybrid nanofluid of covalent functionalized-graphene nanoplatelets (CF-GNPs) with hexagonal boron nitride (h-BN) and covalent functionalized-multi-walled carbon nanotubes (CF-MWCNTs). Experiments were conducted as per ASHRAE standard 93-2010 and the mass flow rate was controlled in the range of 2 to 4 L/min. The efficiency was improved by 85% at a mass flow rate of 4 L/min. Similarly, Tong et al. [88] analyzed the performance characteristics of FPSC by exploiting various nanofluids (Al_2O_3 nanofluid, CuO nanofluid, Fe_3O_4 nano-fluid, and multi-walled carbon nanotube (MWCNT)). The highest efficiency of 87% was reported when MWCNT nanofluid was exploited.

A summary of the various investigations is listed in Table 4 for ready reference.

Table 4. Selective studies on nanofluids.

Authors	Base Fluids	Nanoparticles	Concentrations	Key Results
Yousefi et al. [70]	Water	MWCNT	0.2–0.4% by weight	Particle concentration has a significant effect on efficiency
Yousefi et al. [71]	Water	Al_2O_3	0.2–0.4% by weight	Efficiency was increased up to 28.3%
Heyhat et al. [72]	Distilled Water	Al_2O_3	0.1–2% by volume	Heat transfer coefficient enhanced by 23%.
Alim et al. [74]	Water	Al_2O_3, CuO, SiO_2, TiO_2	1–4% by volume	—
Colangelo et al. [83]	Water	Al_2O_3	1–3% by volume	Convective heat transfer improved by 25%.
Moghadam et al. [75]	Water	CuO	0.4%	Efficiency increased up to 21.8%.
Nasrin et al. [76]	Water	CuO, Al_2O_3, Cu, Ag	0–10%	High particle concentration provided better performance.
Zamzamian et al. [77]	Water	Cu	0.2% and 0.3% by weight	Particle concentration of 0.3% provided optimum efficiency
Colangelo et al. [84]	Water	Al_2O_3	3.0%	High temperatures reported as favorable conditions.
Goudarzi et al. [78]	Water	Al_2O_3 CuO	0.2% for Al_2O_3 0.1% for CuO	Efficiency improved by 52%.
He et al. [80]	Water	CuO	0.1% and 0.2% weight	Efficiency increased up to 24.52%.

Table 4. *Cont.*

Authors	Base Fluids	Nanoparticles	Concentrations	Key Results
Salvati et al. [81]	Water+ethylene glycol	SiO_2	Up to 1%	Efficiency was increased in the range of 4–8%.
Shojaeizadeh et al. [89,90]	Water	Al_2O_3	0–3.5% volume	Maximum exergy efficiency increased by 1%/
Ahmadi et al. [91]	Deionized water	Graphene Nanoplatelets	0.01% and 0.02% weight	Efficiency increased up to 18.87%
Jeon et al. [92]	Water	Al_2O_3	0.1–0.3% volume	Exergy efficiencies and energy increased by 20.3% and 83.5%, respectively.
Verma et al. [93]	Water	Al_2O_3 TiO_2 SiO_2 CuO Grephene MWCNTs	23% for Al_2O_3 35% for TiO_2 30% for SiO_2 18% for CuO 20% for Grephene 20% for MWCNTs	MWCNTs proved maximum energy and exergy efficiencies.
Mirzaei et al. [85]	Water	Al_2O_3	0–1% volume	Efficiency increased up to 23.6%
Kilic et al. [86]	Water	TiO_2	2% wt.	Maximum efficiency was found as 48.67%.
Genc et al. [94]	Water	Al_2O_3	1%, 2% and 3% vol.	Highest thermal efficiency was found as 83.90%.

4.4. Heat Pipe and Mini/Micro Channels

The use of a heat pipe and mini/macro channel in the collector is important due to several advantages, such as a large surface area, high heat transfer coefficient, and small working fluid inventory. However, the fabrication of such collectors is very complex and needs special attention. The blocking of channels is a problematic issue that restricts the use of fluid in mini/micro channels. Researchers have designed and developed the heat pipe and micro/mini flow passages for working fluids and these designs have been efficiently applied to FPSC. Sharma and Diaz [95] improved the performance of a solar collector consisting of micro channel arrays fitted in an absorber tube along their length. The flow rate of the working fluid could be varied from 10^{-3} to 10^{-2} kg/s for better thermal and hydraulic efficiency as recommended. Mansour [96] numerically explored the pressure drop and heat transfer and characteristics of a minichannel-based FPSC. The experimental overall heat loss coefficient and instantaneous efficiency were compared with the numerical results. It was found that the heat removal factor of the novel collector was observed to be 16.1% as compared to the conventional collector.

A novel design of a micro-channel heat pipe array in FPSC (MHPA-FPSC) was presented to enhance the performance by Deng et al. [97]. MHPA-FPSC went through several tests to measure its performance. Aluminum sheets were used to fabricate the micro-channel. Results were obtained in the form of the instantaneous efficiency (η), which is a function of the reduced temperature parameter (Twi–Ti). It was concluded that maximum efficiency of 80% was achieved, which was 11.5% more than the Chinese Standard. Oyinlola et al. [98] studied the performance characteristics of a collector equipped with a micro-channel absorber plate experimentally and theoretically. Microchannels were fabricated using two 340 mm × 240 mm × 10 mm aluminum slabs with a thin channel plate of 3 mm. It was concluded that the temperature profile of the channel could be altered significantly by the effect of axial thermal conduction. Further, Oyinlola et al. [99] improved the thermal and hydraulic performance using a mini-channel. Each collector plate consists of 60 channels of 2 mm wide and 270 mm long. Comparatively, a higher Nusselt number was obtained when the aspect ratio of the channel reached unity. However, the friction factor was observed to be slightly higher than those obtained in a rectangular channel. A large pressure drop was reported in a microchannel or traditional absorber tube as an effect of the working fluid.

Azad [100,101] designed a gravity-based heat pipe fitted with a collector to study the performance in outdoor conditions. A theoretical model was also developed to validate the experimental results. A good accuracy between the experimental results and results predicted by the model was reported. It was recommended that production costs could be reduced by interconnecting heat pipes in the collector. Wei et al. [102] proposed an improved structure of FPSC. The novel collector is integrated with a wickless heat pipe. It was shown that the maximum efficiency reached up to 66% and the water temperature in a 200 liter tank increased by 25 °C. A similar study of FPSC with MHPA was proposed by Zhu et al. [103]. The heat loss, outlet temperature, heat transfer, and thermal efficiency were evaluated under different weather conditions. It was reported that the average efficiency increased up to 69%. A solar collector was designed, which utilized the combined effect of a flat micro-heat pipe array (FMHPA) and vacuum technology [104]. Aluminum fins attached to the other ends of the heat pipe were exploited to increase the heat transfer to flow fluid. It was reported that the collector efficiency reached up to 73% in the summer seasons. Ersoz [105] investigated the behavior of a thermosyphon heat pipe integrated with evacuated tube solar collectors in regards to the energy and exergy performance. Various fluids, i.e., ethanol, methanol, acetone, hexane, petroleum ether, and chloroform, were tested using the same specifications. It was reported that the highest exergy and energy efficiencies were obtained when acetone was used as the working fluids.

Zhang et al. [106] explored the performance of FPSC equipped with a heat pipe under steady-state conditions. The model of this novel collector consisted of a cross-flow heat exchanger and shell, glass cover, insulation layer, absorber plate, and two-phase closed thermosyphon. The average useful heat gain could be improved by increasing the absorber plate thickness and evaporator length. Additionally, an inclined angle from 30° to 45° was recommended when the collector faced the south direction. Wang et al. [107] designed two flat micro-heat pipe arrays (FMHPA)-based FPSC, i.e., transparent-tube collector (T-TC) and conventional-tube collector (C-TC), in which FMHPA acts as the core heat transfer element for both collectors. The thermal efficiency and useful energy gain of C-TC were 77.6% and 641 W, respectively. However, the thermal efficiency and useful energy gain of T-TC were 85% and 497 W, respectively. The overall performance of C-TC was significant in comparison to T-TC, as reported. Table 5 presents the key findings of the heat pipe and mini/macro channel in FPSC for ready reference.

Table 5. Selective study of the heat pipe and mini/micro channel used in the collector.

Authors	Description	Study Type	Parameters	Key Results
Azad [100]	Gravity assisted heat pipe collector	Both Theoretically and Experimentally	M = 0.03–0.032 kg/s, Number of heat pipe = 6	Heated length-cooled length ratio was optimized.
Azad [101]	Three different heat pipe collector were tested	Experimental	—	Cost could be reduced by interconnecting all heat pipe.
Wei et al. [102]	collector was integrated with wickless heat pipe	Experimental and Theoretical Both	m = 0.2 kg/s, Ti = 25.2 °C	Collector efficiency improved up to 66%.
Zhu et al. [104]	Combined effect of flat micro-heat pipes array (FMHPA) and vacuum technology	Experimental	Radiation as function of time	Maximum efficiency was reported as 69%.
Ersoz [105]	Effect of six different working fluids in evacuated tube solar collectors	Experimental	—	Out of six working fluids, acetone and chloroform showed the best exergy performance.
Zhang et al. [106]	FPSC with heat pipe	Numerical	Heat pipe length = 605–900 mm, Plate thickness = 0.1–2.2 mm, Heat pipe dia = 8–16 mm	Length and thickness of the collector significantly affected the performance

4.5. Vacuum Collector

FPSCs have high heat loss through their top glass covers, which means they cannot operate with lower efficiencies at temperatures over 100 °C. This problem could be overcome by creating a vacuum around the absorber, which leads to the advantages of elimination of convective heat losses due to the high insulating properties of the vacuum [108,109]. Vacuum FPSCs have a great advantages, which include excellent thermal characteristics and optical properties due to a combination of high vacuum thermal insulation and their wide surface area [110]. However, maintaining the vacuum in FPSC is a major challenge that depends on the materials used in fabrication, forming a durable hermetic seal around the periphery of the vacuum [111]. In order to eliminate convective losses, several researchers have directed their studies by creating a vacuum around the absorber. Eaton and Blum [108] theoretically investigated the vacuum flat plate collector to eliminating the natural convection losses from the absorber plate to the cover. Later on, Benz and Beikircher [109] produced steam by developing a prototype of FPSC. Convection losses were reduced significantly due to partial evacuation to about 1000 Pa; however, gas conduction still fully developed, which led to thermal loss. Gas conductance losses decreased with a decrease in the vacuum pressure, which could help to achieve a higher absorber plate temperature.

Buttinger et al. [112] developed an edge ray collector filled with low pressure inert gas to reduce the convention losses. In order to increase the radiation on headers, asymmetric reflectors were placed below the headers to minimize the longitudinal radiation losses and to maximize the incoming solar radiation. Convection losses were prevented inside the tube by keeping the pressure of inert gas (krypton) below 10 mbar. This prototype showed 50% efficiencies at a temperature of 150 °C and pressure of 0.01 bar. Maintaining the vacuum was challenging because a durable hermitic seal around the periphery panel was very crucial. Vacuum panels were fabricated using a hermetic seal. This hermetic seal was created with a metal alloy, such as indium or Cerasolzer 217 using the ultra soldering technique in Ulster and Loughborough University [113,114]. TVP-Solar fabricated commercially fabricated the vacuum flat plate collector. The high-vacuum insulation completely suppressed convection losses inside the panels and enabled a conversion efficiency of above 70%. The thickness of the absorber plate is 0.2 mm and the collector has an aperture area of about 1 m^2. Glass can safely withstand atmospheric pressures using a lightweight support structure [115]. CERN developed an ultra-vacuum collector, which can achieve a maximum temperature of 350 °C [116]. Henshall et al. [117] analyzed the mechanically stressed vacuum collector enclosure when it was subjected to atmospheric pressure loading and differential thermal expansion of dissimilar components.

In order to present the global scenario, various performance improvement techniques were analyzed and discussed in the previous sub-section. The efficiency of FPSC exploiting different techniques is shown in the radar graph (Figure 5). Each graph shows the efficiency of only one functional parameter studied by different researchers. It is very difficult to shows the results of all studies in terms of efficiency due to the lack of data published in corresponding papers. It can be seen from the graph that geometrical modification have the least effect on efficiency improvement and a convergent-divergent absorber tube could improve the efficiency by around 42% [58]; however, porous disc inserts result in a substantial improvement in efficiency [31]. The effect of nanofluid on efficiency has a wide range due to various parameters like the thermal properties of nanoparticles, base fluids, flow configurations, and system parameters of the collector arrangements. Out of many nanofluids, MWCNT nanofluids have the most significant results, as an efficiency of around 87% was reported [89]. Additionally, CuO nanofluid exhibited significant efficiency of 85% followed by MWCNT nanofluids, and a high performance of CuO nanofluids was achieved due to the high thermal conductivity of Cu nanoparticles [76]. The use of heat pipes/micro heat channels is also effective, and efficiencies of 66% and 69% were reported for a wickless heat pipe and microchannel [74,76]. Results of the solar selective coating have been published in terms of the absorptivity and emissivity of various FPSC, so it is difficult to quantify the results in terms of efficiency. However, an efficiency of a collector with black chrome coating of 30% more efficient in comparison to a collector with conventional coating was reported [46]. However, the absolute efficiency (52%) of the collector with black chrome coating was estimated by considering the 40% efficiency of the collector with conventional coating and is shown in Figure 5. The inference from the various performance improvement techniques is summarized in Table 6.

Geometrical Modifications	Convergent-divergent absorber tube [58] Porous disc inserts [30]
Solar Selective Coating	Blcak chrome coating [46]
Nano-Fluids	Al_2O_3 nano-particles in water [63] CuO/water nanofluid [68] CuO nanoparticles in helical tube [72] CuO nanoparticles in water [71] SiO_2 nanoparticles in water+ethylene glycol [74] Graphene nano-partcles [84] MWCNT nano-fluid [81] TiO_2/water nanofluid [79]
Heat Pipe	Wickless heat pipe [102] Micro-heat pipes array [103]

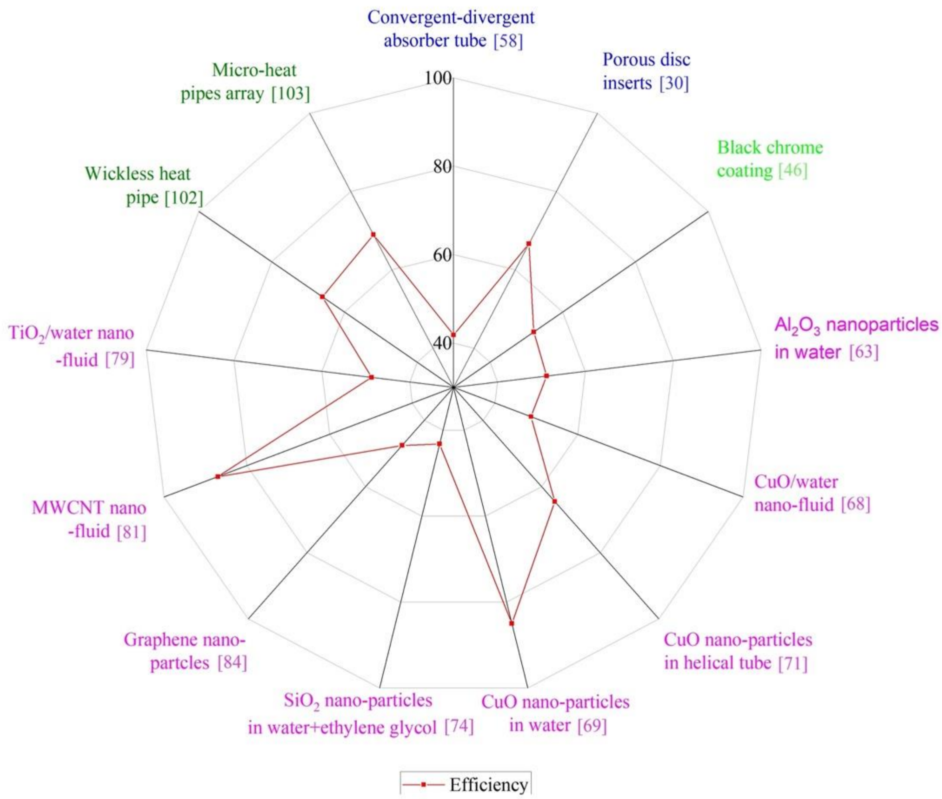

Figure 5. Comparison of efficiency exploiting different techniques.

Table 6. Inferences from the various performance improvement techniques.

S.No.	Techniques	Advantages	Disadvantages	Inference from Studies
1	Geometrical modifications	Thermal performance increases with increase in heat transfer without compromising with size or maintaining the compact size.	Turbulence is responsible for high pressure drop penalty which requires additional pumping power.	The aim of geometrical modification is to increase the Nu number without increasing pressure drop. Helical screw tape inserts were promising to reduce the heat loss. Metal foam inserts improved the Nusselt number many folds. Coil wire turbulators could substantially increase the heat transfer without increasing pumping power. Due to turbulators, rate of heat transfer enchantment decreased with increase of mass flow rate/Reynolds number.
2	Use of nanofluids	Nanofluids have high heat extraction rate from the collector due to its high heat conductivities and heat carrying capacities	Aggregation and sedimentation of nanoparticles in nanofluids are major issue, these fluids should be stable.	Nanoparticle concentrations have significant effect on the collector performance. Collector performance increases with increase in nano particle concentration and decreases with increase in nanoparticles sizes. Among different nanofluids, CuO/water and MWCNT nanofluid have highest heat transfer potential.
3	Solar Selective Coatings	Solar selective coating helps to harness the maximum amount of insolation along. Stability of solar selective coatings are good over collector lifetime.	The performance of solar selective coating decreases with over its life. Absorption rate of coating decreased up to 2% in a year.	The coating of $V{:}Al_2O_3$ has superior optical properties. The solar absorptance and emittance were found to be 0.98 and 0.02, respectively. The nickel-pigmented aluminum oxide is have better characteristic due to its highly conversion efficiency and high durability.
4	Heat pipe and Mini/Micro channel	These heat pipe and mini/macro channels have high heat transfer rate, small working fluid inventory, and high convective heat transfer coefficient.	The blocking of channels are major challenges. The manufacturing cost are high that restrict the usage of such channels.	Collectors equipped with heat pipe have high sensitivity to temperature and have high conversion efficiency. Additionally, macro/mini channel-based collectors have high heat collector efficiency due to its high heat removal factor.
5	Vacuum Collectors	Vacuum around absorbers suppresses the convective heat loss and leading to higher heat gain and conversion efficiency.	The major challenge is hermitic seal to maintain the vacuum. The expansion and contraction of the pane cover, and assembly affect the strength of hermitic seal due to wide range of temperature variation	The conversion efficiency of these collectors is above 70%. The indium alloy edge seal allows to fabricate vacuum sealing at low temperature in a vacuum chamber

5. Conclusions

In this paper, STCs were categorized on the basis of their movement about the axis, and their corresponding efficiency, working temperature range, and applications were listed. Performance improvement techniques were identified and discussed in detail. These techniques focus on performance improvement using turbulators, the nature of working fluids (nanofluids, etc.), solar selective coating, heat pipe, micro/mini channel, and vacuum around absorber. Based on the discussion on each technique, the following conclusions can be made:

- The turbulators/surface modifications in the absorber tube are strongly recommended for enhancing the convective heat transfer coefficient. Dimple roughness is found to be hydraulically better, but it is not thermally viable to address the performance improvement. Although, a metal foam insert could enhance the Nusselt number by 5–10 times. The Nusselt number could also be increased by insertion of a wire mesh, coil, and twisted tapes. Particular surface modification/inserts can be utilized and designs are based on the requirement of the system, e.g., outlet temperature of working fluids. Additional inserts/elements lead to a pressure drop, which is a major drawback
- Solar selective coatings are the better way to improve the performance significantly. These coatings may also help to increase the life of a collector. Selective coating of $Cu_{0.44}$ $Ti_{0.44}$ $Mn_{0.84}$ helps to absorb up to 97.4% of the incident solar energy and com-

bined with a black chrome on nickel-plated copper substrate showed an absorptivity of 0.96. Although, the major drawbacks associated with selective coatings are the comparatively high cost and the complexity in the production process, which restricts commercial usage.

- The performance is also dependent on the choice of working temperature and conductivity of the working temperature. Generally, refrigerants (like HFC (R245fa), HCFC (R123)), mixture of water and glycol and paraffinic hydrocarbon oils, and/or a eutectic mixture of synthetic compounds are used for low-, medium-, and high-temperature applications, respectively. Nanofluid is an alternate and the best solution in a solar collector because the thermal conductivity of the nanofluid can controlled. Therefore, the use of nanofluids was emphasized in this paper. MWCNT nanofluids exhibited significant efficiency, i.e., 87%. The addition of nanoparticles can improve the thermal conductivity, which leads to performance improvement, although sedimentation is a major issue, which can be resolved by modifying the manifold/channeling.
- Use of a mini/macro channel and heat pipes is very economical because it requires low fluid inventory. Mini/macro channels are very effective for improving heat transfer. A HPA collector with aluminum fins can improve the efficiency up to 73% and 66% efficiency is achieved in the case of a collector integrated with a wickless heat pipe at a low flow rate (0.2 kg/s). However, the design of a mini/macro channel is very complex due to several parameters involved in it. Chocking of the channel is the major issue that restricts fluid flow.
- Vacuum in a collector is a promising technology, which can substantially suppress the convection losses around the absorber and enable to a high conversion efficiency above 70% and can supply heat around 350 °C.

Hence, it is concluded that the research work carried out by several researchers shows a deep interest in the topic and there are several ways to develop an efficient and compact flat plate solar collector. The FPSCs are not only cheap but also environment friendly. However, there is a need to explore those techniques that are not only make an efficient FPSC but also make it compact and can be used in cloudy weather/low sunshine conditions.

6. Challenges and Future Recommendation

The vacuum in the collector is considered to be a very promising technology; however, there are many challenges in its fabrication. The major challenges are the hermetic seal to maintain the vacuum against atmospheric pressure, thermal expansion, and contraction of pane coves, which substantially reduce the strength of the hermitic seal over its life time. Additionally, maintaining the gaps between the absorber and glass pan to eliminate conductive heat losses under the influence of atmospheric pressure is more challenging.

Further, the future research aims may be to develop evacuated or inert gas-filled FPSC, which would reduce the convective losses, leading to higher performance as compared to the listing systems/technologies

Author Contributions: Conceptualization, T.A. and N.B.B.; methodology, T.A., K.S.K. and R.C.; software, M.I.H.S.; validation, T.A., N.B.B. and N.R.K.; formal analysis, T.A.; investigation, N.B.B.; resources, T.A., K.S.K.; data curation, N.R.K.; writing—original draft preparation, T.A., R.C. and A.K.; writing—review and editing, T.A., R.C., C.S.M. and A.K.; visualization, C.S.M., M.I.H.S. and R.C.; supervision, T.A. and R.C.; project administration, T.A. and A.K. All authors have read and agreed to the published version of the manuscript.

Funding: This research received no external funding.

Data Availability Statement: The data are not publicly available due to privacy considerations.

Conflicts of Interest: The authors declare no conflict of interest.

References

1. Esen, M. Thermal performance of a solar cooker integrated vacuum-tube collector with heat pipes containing different refrigerants. *Sol. Energy* **2004**, *76*, 751–757. [CrossRef]
2. Esen, M.; Esen, H. Experimental investigation of a two-phase closed thermosyphon solar water heater. *Sol. Energy* **2005**, *79*, 459–468. [CrossRef]
3. Alam, T.; Saini, R.P.; Saini, J.S. Heat Transfer Enhancement due to V-Shaped Perforated Blocks in a Solar Air Heater Duct. *Appl. Mech. Mater.* **2014**, *619*, 125–129. [CrossRef]
4. Alam, T.; Kim, M. Numerical study on thermal hydraulic performance improvement in solar air heater duct with semi ellipse shaped obstacles. *Energy* **2016**, *112*, 588–598. [CrossRef]
5. Zayed, M.E.; Zhao, J.; Elsheikh, A.H.; Du, Y.; Hammad, F.A.; Ma, L.; Kabeel, A.E.; Sadek, S. Performance augmentation of flat plate solar water collector using phase change materials and nanocomposite phase change materials: A review. *Process Saf. Environ. Prot.* **2019**, *128*, 135–157. [CrossRef]
6. Esen, M.; Yuksel, T. Experimental evaluation of using various renewable energy sources for heating a greenhouse. *Energy Build.* **2013**, *65*, 340–351. [CrossRef]
7. Esen, H.; Esen, M.; Ozsolak, O. Modelling and experimental performance analysis of solar-assisted ground source heat pump system. *J. Exp. Theor. Artif. Intell.* **2017**, *29*, 1–17. [CrossRef]
8. Sharma, V.; Kumar, A.; Sastry, O.S.; Chandel, S.S. Performance assessment of different solar photovoltaic technologies under similar outdoor conditions. *Energy* **2013**, *58*, 511–518. [CrossRef]
9. Al-Harahsheh, M.; Abu-Arabi, M.; Mousa, H.; Alzghoul, Z. Solar desalination using solar still enhanced by external solar collector and PCM. *Appl. Therm. Eng.* **2018**, *128*, 1030–1040. [CrossRef]
10. Sukhatme, S.P. *Solar Energy: Principles of Thermal Collection and Storage*, 9th ed.; Tata McGraw-Hill: New Delhi, India, 2003.
11. Suman, S.; Khan, M.K.; Pathak, M. Performance enhancement of solar collectors—A review. *Renew. Sustain. Energy Rev.* **2015**, *49*, 192–210. [CrossRef]
12. Kalogirou, S.A. Solar Thermal Collectors and Applications. *Prog. Energy Combust. Sci.* **2004**, *30*(1), 231–295. [CrossRef]
13. Said, Z.; Sundar, L.S.; Tiwari, A.K.; Ali, H.M.; Sheikholeslami, M.; Bellos, E.; Babar, H. Recent advances on the fundamental physical phenomena behind stability, dynamic motion, thermophysical properties, heat transport, applications, and challenges of nanofluids. *Phys. Rep.* **2021**, 2–4. [CrossRef]
14. Said, Z.; Hachicha, A.A.; Aberoumand, S.; Yousef, B.A.A.; Sayed, E.T.; Bellos, E. Recent advances on nanofluids for low to medium temperature solar collectors: Energy, exergy, economic analysis and environmental impact. *Prog. Energy Combust. Sci.* **2021**, *84*, 2–5. [CrossRef]
15. Jebaraj, S.; Al-Qahtani, A.M. A review on performance, heat transfer and exergy analysis of solar flat plate collectors. *World Rev. Sci. Technol. Sustain. Dev.* **2021**, *17*, 114687. [CrossRef]
16. Available online: http://www.paksolarservices.com/solar-heat-collector.html (accessed on 16 August 2021).
17. Alam, T.; Meena, C.S.; Balam, N.B.; Kumar, A.; Cozzolino, R. Thermo-Hydraulic Performance Characteristics and Optimization of Protrusion Rib Roughness in Solar Air Heater. *Energies* **2021**, *14*, 3159. [CrossRef]
18. Hobbi, A.; Siddiqui, K. Experimental study on the effect of heat transfer enhancement devices in flat-plate solar collectors. *Int. J. Heat Mass Transf.* **2009**, *52*, 4435–4448. [CrossRef]
19. Mwesigye, A.; Bello-Ochende, T.; Meyer, J.P. Heat transfer and thermodynamic performance of a parabolic trough receiver with centrally placed perforated plate inserts. *Appl. Energy* **2014**, *136*, 989–1003. [CrossRef]
20. Şahin, H.M.; Baysal, E.; Dal, A.R.; Şahin, N. Investigation of heat transfer enhancement in a new type heat exchanger using solar parabolic trough systems. *Int. J. Hydrogen Energy* **2015**, *40*, 15254–15266. [CrossRef]
21. Fuqiang, W.; Qingzhi, L.; Huaizhi, H.; Jianyu, T. Parabolic trough receiver with corrugated tube for improving heat transfer and thermal deformation characteristics. *Appl. Energy* **2016**, *164*, 411–424. [CrossRef]
22. Fuqiang, W.; Zhexiang, T.; Xiangtao, G.; Jianyu, T.; Huaizhi, H.; Bingxi, L. Heat transfer performance enhancement and thermal strain restrain of tube receiver for parabolic trough solar collector by using asymmetric outward convex corrugated tube. *Energy* **2016**, *114*, 275–292. [CrossRef]
23. Song, X.; Dong, G.; Gao, F.; Diao, X.; Zheng, L.; Zhou, F. A numerical study of parabolic trough receiver with nonuniform heat flux and helical screw-tape inserts. *Energy* **2014**, *77*, 771–782. [CrossRef]
24. Wang, P.; Liu, D.Y.; Xu, C. Numerical study of heat transfer enhancement in the receiver tube of direct steam generation with parabolic trough by inserting metal foams. *Appl. Energy* **2013**, *102*, 449–460. [CrossRef]
25. Zheng, Z.J.; Li, M.J.; He, Y.L. Thermal analysis of solar central receiver tube with porous inserts and non-uniform heat flux. *Appl. Energy* **2015**, *185*, 1151–1161. [CrossRef]
26. Martín, R.H.; Pérez-García, J.; García, A.; García-Soto, F.J.; López-Galiana, E. Simulation of an enhanced flat-plate solar liquid collector with wire-coil insert devices. *Sol. Energy* **2011**, *85*, 455–469. [CrossRef]
27. Axtmann, M.; Poser, R.; Von Wolfersdorf, J.; Bouchez, M. Endwall heat transfer and pressure loss measurements in staggered arrays of adiabatic pin fins. *Appl. Therm. Eng.* **2016**, *103*, 1048–1056. [CrossRef]
28. Chin, S.-B.; Foo, J.-J.; Lai, Y.-L.; Yong, T.K.-K. Forced convective heat transfer enhancement with perforated pin fins. *Heat Mass Transf.* **2013**, *49*, 1447–1458. [CrossRef]

29. Gong, X.; Wang, F.; Wang, H.; Tan, J.; Lai, Q.; Han, H. Heat transfer enhancement analysis of tube receiver for parabolic trough solar collector with pin fin arrays inserting. *Sol. Energy* **2017**, *144*, 185–202. [CrossRef]
30. Reddy, K.S.; Ravi Kumar, K.; Ajay, C.S. Experimental investigation of porous disc enhanced receiver for solar parabolic trough collector. *Renew. Energy* **2015**, *77*, 308–319. [CrossRef]
31. San, J.; Huang, W.; Chen, C. Experimental investigation on heat transfer and fluid friction correlations for circular tubes with coiled-wire inserts. *Int. Commun. Heat Mass Transf.* **2015**, *65*, 8–14. [CrossRef]
32. Jamal-Abad, M.T.; Saedodin, S.; Aminy, M. Experimental investigation on a solar parabolic trough collector for absorber tube fi lled with porous media. *Renew. Energy* **2017**, *107*, 156–163. [CrossRef]
33. Rassamakin, B.; Khairnasov, S.; Zaripov, V.; Rassamakin, A.; Alforova, O. Aluminum heat pipes applied in solar collectors. *Sol. Energy* **2013**, *94*, 145–154. [CrossRef]
34. Sandhu, G.; Siddiqui, K.; Garcia, A. Experimental study on the combined effects of inclination angle and insert devices on the performance of a flat-plate solar collector. *Int. J. Heat Mass Transf.* **2014**, *71*, 251–263. [CrossRef]
35. García, A.; Herrero-Martin, J.P.; Solano, J.; Perez-Garcia, J. The role of insert devices on enhancing heat transfer in a flat-plate solar water collector. *Appl. Therm. Eng.* **2018**, *132*, 479–489. [CrossRef]
36. Balaji, K.; Iniyan, S.; Swami, M.V. Exergy, economic and environmental analysis of forced circulation flat plate solar collector using heat transfer enhancer in riser tube. *J. Clean. Prod.* **2018**, *171*, 1118–1127. [CrossRef]
37. Anirudh, K.; Dhinakaran, S. Performance improvement of a flat-plate solar collector by inserting intermittent porous blocks. *Renew. Energy* **2020**, *145*, 428–441. [CrossRef]
38. Anirudh, K.; Dhinakaran, S. Numerical study on performance improvement of a flat-plate solar collector filled with porous foam. *Renew. Energy* **2020**, *147*, 1704–1717. [CrossRef]
39. Fan, M.; Zheng, W.; You, S.; Zhang, H.; Jiang, Y.; Wu, Z. Comparison of different dynamic thermal performance prediction models for the flat-plate solar collector with a new V-corrugated absorber. *Sol. Energy* **2020**, *204*, 406–418. [CrossRef]
40. Gao, M.; Wang, D.; Liu, Y.; Wang, Y.; Zhou, Y. A study on thermal performance of a novel glazed transpired solar collector with perforating corrugated plate. *J. Clean. Prod.* **2020**, *257*, 120443. [CrossRef]
41. Shaffer, L.H. Wavelength-dependent (selective) processes for the utilization of solar energy. *Sol. Energy* **1958**, *2*, 21–26. [CrossRef]
42. Chen, D. Anti-reflection (AR) coatings made by sol gel processes: A review. *Sol. Energy Mater. Sol. Cells* **2001**, *68*, 313–336. [CrossRef]
43. Coatirg, S.; Kaushal, D.K. An overview of solar thermal devices based solar water heating systems & the nesessity of using solar selective coating. *Renew. Energy* **1997**, *10*, 355–361.
44. Cindrella, L. The real utility ranges of the solar selective coatings. *Sol. Energy Mater. Sol. Cells* **2007**, *91*, 1898–1901. [CrossRef]
45. Tulchinsky, D.; Uvarov, V.; Popov, I.; Mandler, D.; Magdassi, S. A novel non-selective coating material for solar thermal potential application formed by reaction between sol-gel titania and copper manganese spinel. *Sol. Energy Mater. Sol. Cells* **2014**, *120*, 23–29. [CrossRef]
46. Abbas, A. Solchrome solar selective coatings—An effective way for solar water heates globally. *Renew. Energy* **2000**, *19*, 145–154. [CrossRef]
47. Schuler, A.; Videnovic, I.R.; Oelhafen, P.; Brunold, S. Titanium-containing amorphous hydrogenated silicon carbon films (a-Si:C:H/Ti) for durable solar absorber coatings. *Sol. Energy Mater. Sol. Cells* **2001**, *69*, 271–284. [CrossRef]
48. Teixeira, V.; Sousa, E.; Costa, M.F.; Nunes, C.; Rosa, L.; Carvalho, M.J.; Collares-Pereira, M.; Roman, E.; Gago, J. Spectrally selective composite coatings of Cr-Cr2O3 and Mo-Al2O3 for solar energy applications. *Thin Solid Films* **2001**, *392*, 320–326. [CrossRef]
49. Farooq, M.; Hutchins, M.G. Optical properties of higher and lower refractive index composites in solar selective coatings. *Sol. Energy Mater. Sol. Cells* **2002**, *71*, 73–83. [CrossRef]
50. Farooq, M.; Hutchins, M.G. A novel design in composites of various materials for solar selective coatings. *Sol. Energ. Mater. Sol. C* **2002**, *71*, 523–535. [CrossRef]
51. Shashikala, A.R.; Sharma, A.K.; Bhandari, D.R. Solar selective black nickel-cobalt coatings on aluminum alloys. *Sol. Energy Mater. Sol. Cells* **2007**, *91*, 629–635. [CrossRef]
52. Wazwaz, A.; Salmi, J.; Bes, R. The effects of nickel-pigmented aluminium oxide selective coating over aluminium alloy on the optical properties and thermal efficiency of the selective absorber prepared by alternate and reverse periodic plating technique. *Energy Convers. Manag.* **2010**, *51*, 1679–1683. [CrossRef]
53. Juang, R.C.; Yeh, Y.C.; Chang, B.H.; Chen, W.C.; Chung, T.W. Preparation of solar selective absorbing coatings by magnetron sputtering from a single stainless steel target. *Thin Solid Films* **2010**, *518*, 5501–5504. [CrossRef]
54. Du, M.; Liu, X.; Hao, L.; Wang, X.; Mi, J.; Jiang, L.; Yu, Q. Microstructure and thermal stability of Al/Ti0.5Al0.5N/Ti0.25Al0.75N/AlN solar selective coating. *Sol. Energy Mater. Sol. Cells* **2013**, *111*, 49–56. [CrossRef]
55. Du, M.; Hao, L.; Mi, J.; Lv, F.; Liu, X.; Jiang, L.; Wang, S. Optimization design of Ti0.5Al0.5N/Ti0.25Al0.75N/AlN coating used for solar selective applications. *Sol. Energy Mater. Sol. Cells* **2011**, *95*, 1193–1196. [CrossRef]
56. Nuru, Z.Y.; Arendse, C.J.; Muller, T.F.; Khamlich, S.; Maaza, M. Thermal stability of electron beam evaporated AlxO y/Pt/AlxOy multilayer solar absorber coatings. *Sol. Energy Mater. Sol. Cells* **2014**, *120*, 473–480. [CrossRef]
57. Nuru, Z.Y.; Arendse, C.J.; Khamlich, S.; Maaza, M. Optimization of AlxOy/Pt/AlxOy multilayer spectrally selective coatings for solar–thermal applications. *Vacuum* **2012**, *86*, 2129–2135. [CrossRef]

58. Khamlich, S.; McCrindle, R.; Nuru, Z.Y.; Cingo, N.; Maaza, M. Annealing effect on the structural and optical properties of Cr/??-Cr2O3 monodispersed particles based solar absorbers. *Appl. Surf. Sci.* **2013**, *265*, 745–749. [CrossRef]
59. Karthick Kumar, S.; Murugesan, S.; Suresh, S. Preparation and characterization of CuO nanostructures on copper substrate as selective solar absorbers. *Mater. Chem. Phys.* **2014**, *143*, 1209–1214. [CrossRef]
60. Liu, H.D.; Wan, Q.; Lin, B.Z.; Wang, L.L.; Yang, X.F.; Wang, R.Y.; Gong, D.Q.; Wang, Y.B.; Ren, F.; Chen, Y.M.; et al. The spectral properties and thermal stability of CrAlO-based solar selective absorbing nanocomposite coating. *Sol. Energy Mater. Sol. Cells* **2014**, *122*, 226–232. [CrossRef]
61. Valleti, K.; Murali Krishna, D.; Joshi, S.V. Functional multi-layer nitride coatings for high temperature solar selective applications. *Sol. Energy Mater. Sol. Cells* **2014**, *121*, 14–21. [CrossRef]
62. Céspedes, E.; Wirz, M.; Sánchez-García, J.A.; Alvarez-Fraga, L.; Escobar-Galindo, R.; Prieto, C. Novel Mo-Si_3N_4 based selective coating for high temperature concentrating solar power applications. *Sol. Energy Mater. Sol. Cells* **2014**, *122*, 217–225. [CrossRef]
63. Tsai, T.K.; Li, Y.H.; Fang, J.S. Spectral properties and thermal stability of CrN/CrON/Al_2O_3 spectrally selective coating. *Thin Solid Films* **2016**, *615*, 91–96. [CrossRef]
64. Schhuler, A.; Geng, J.; Oelhafen, P.; Brunold, S.; Gantenbein, P.; Frei, U. Application of titanium containing amorphous hydrogenated carbon films (a-C:H/Ti) as optical selective solar absorber coatings. *Sol. Energy Mater. Sol. Cells* **2000**, *60*, 295–307. [CrossRef]
65. Li, H.; Lu, S.; Li, Y.; Qin, W.; Wu, X. Tunable thermo-optical performance promoted by temperature selective sputtering of titanium oxide on MgO-ZrO_2 coating. *J. Alloys Compd.* **2017**, *709*, 104–111. [CrossRef]
66. Srivastva, U.; Malhotra, R.K.; Kaushik, S.C. Recent Developments in Heat Transfer Fluids Used for Solar Thermal Energy Applications Fundamentals of Renewable Energy and Applications. *J. Renew. Energy Appl.* **2015**, *5*(6), 1000189. [CrossRef]
67. Ranjith, P.V.; Karim, A.A. A Comparative Study on the Experimental and Computational Analysis of Solar Flat Plate Collector using an Alternate Working Fluid. *Procedia Technol.* **2016**, *24*, 546–553. [CrossRef]
68. Xuan, Y.; Li, Q. Heat transfer enhancement of nanofluids. *Int. J. Heat Fluid Flow* **2000**, *21*, 58–64. [CrossRef]
69. Colangelo, G.; Favale, E.; de Risi, A.; Laforgia, D. Results of experimental investigations on the heat conductivity of nanofluids based on diathermic oil for high temperature applications. *Appl. Energy* **2012**, *97*, 828–833. [CrossRef]
70. Yousefi, T.; Veisy, F.; Shojaeizadeh, E.; Zinadini, S. An experimental investigation on the effect of MWCNT-H_2O nanofluid on the efficiency of flat-plate solar collectors. *Exp. Therm. Fluid Sci.* **2012**, *39*, 207–212. [CrossRef]
71. Yousefi, T.; Veysi, F.; Shojaeizadeh, E.; Zinadini, S. An experimental investigation on the effect of Al_2O_3-H_2O nanofluid on the efficiency of flat-plate solar collectors. *Renew. Energy* **2012**, *39*, 293–298. [CrossRef]
72. Heyhat, M.M.; Kowsary, F.; Rashidi, A.M.; Alem Varzane Esfehani, S.; Amrollahi, A. Experimental investigation of turbulent flow and convective heat transfer characteristics of alumina water nanofluids in fully developed flow regime. *Int. Commun. Heat Mass Transf.* **2012**, *39*, 1272–1278. [CrossRef]
73. Chaji, H.; Ajabshirchi, Y.; Esmaeilzadeh, E.; Heris, S.Z.; Hedayatizadeh, M.; Kahani, M. Experimental study on thermal efficiency of flat plate solar collector using TiO_2/water nanofluid. *Mod. Appl. Sci.* **2013**, *7*, 60–69. [CrossRef]
74. Alim, M.A.; Abdin, Z.; Saidur, R.; Hepbasli, A.; Khairul, M.A.; Rahim, N.A. Analyses of entropy generation and pressure drop for a conventional flat plate solar collector using different types of metal oxide nanofluids. *Energy Build.* **2013**, *66*, 289–296. [CrossRef]
75. Moghadam, A.J.; Farzane-Gord, M.; Sajadi, M.; Hoseyn-Zadeh, M. Effects of CuO/water nanofluid on the efficiency of a flat-plate solar collector. *Exp. Therm. Fluid Sci.* **2014**, *58*, 9–14. [CrossRef]
76. Nasrin, R.; Parvin, S.; Alim, M.A. Heat transfer by nanofluids through a flat plate solar collector. *Procedia Eng.* **2014**, *90*, 364–370. [CrossRef]
77. Zamzamian, A.; Keyanpour Rad, M.; Kiani Neyestani, M.; Jamal-Abad, M.T. An experimental study on the effect of Cu-synthesized/EG nanofluid on the efficiency of flat-plate solar collectors. *Renew. Energy* **2014**, *71*, 658–664. [CrossRef]
78. Goudarzi, K.; Nejati, F.; Shojaeizadeh, E.; Asadi Yousef-Abad, S.K. Experimental study on the effect of pH variation of nanofluids on the thermal efficiency of a solar collector with helical tube. *Exp. Therm. Fluid Sci.* **2015**, *60*, 20–27. [CrossRef]
79. Tomy, A.M.; Ahammed, N.; Subathra, M.S.P.; Asirvatham, L.G. Analysing the Performance of a Flat Plate Solar Collector with Silver/Water Nanofluid Using Artificial Neural Network. *Procedia Comput. Sci.* **2016**, *93*, 33–40. [CrossRef]
80. He, Q.; Zeng, S.; Wang, S. Experimental investigation on the efficiency of flat-plate solar collectors with nanofluids. *Appl. Therm. Eng.* **2014**, *88*, 165–171. [CrossRef]
81. Salavati, S.; Kianifar, A.; Niazmand, H.; Mahian, O.; Wongwises, S. Experimental investigation on the thermal efficiency and performance characteristics of a flat plate solar collector using SiO_2/EG–water nanofluids. *Int. Commun. Heat Mass Transf.* **2015**, *65*, 71–75. [CrossRef]
82. Said, Z.; Saidur, R.; Sabiha, M.A.; Hepbasli, A.; Rahim, N.A. Energy and exergy efficiency of a flat plate solar collector using pH treated Al2O3 nanofluid. *J. Clean. Prod.* **2016**, *112*, 3915–3926. [CrossRef]
83. Colangelo, G.; Favale, E.; De Risi, A.; Laforgia, D. A new solution for reduced sedimentation flat panel solar thermal collector using nanofluids. *Appl. Energy* **2013**, *111*, 80–93. [CrossRef]
84. Colangelo, G.; Favale, E.; Miglietta, P.; de Risi, A.; Milanese, M.; Laforgia, D. Experimental test of an innovative high concentration nanofluid solar collector. *Appl. Energy* **2015**, *154*, 874–881. [CrossRef]
85. Mirzaei, M.; Mohammad, S.; Hosseini, S.; Mansour, A.; Kashkooli, M. Assessment of Al2O3 nanoparticles for the optimal operation of the fl at plate solar collector. *Appl. Therm. Eng.* **2018**, *134*, 68–77. [CrossRef]

86. Kiliç, F.; Menlik, T.; Sözen, A. Effect of titanium dioxide/water nano fluid use on thermal performance of the flat plate solar collector. *Sol. Energy* **2018**, *164*, 101–108. [CrossRef]
87. Harrison, N.A.; Cercignani, M.; Voon, V.; Critchley, H.D. Effects of Inflammation on Hippocampus and Substantia Nigra Responses to Novelty in Healthy Human Participants. *Neuropsychopharmacology* **2015**, *40*, 831–838. [CrossRef]
88. Tong, Y.; Chi, X.; Kang, W.; Cho, H. Comparative investigation of efficiency sensitivity in a flat plate solar collector according to nanofluids. *Appl. Therm. Eng.* **2020**, *174*, 115346. [CrossRef]
89. Shojaeizadeh, E.; Veysi, F.; Kamandi, A. Exergy efficiency investigation and optimization of an Al_2O_3/water nanofluid based Flat-plate solar collector. *Energy Build.* **2015**, *101*, 12–23. [CrossRef]
90. Shojaeizadeh, E.; Veysi, F. Development of a correlation for parameter controlling using exergy efficiency optimization of an Al_2O_3/water nanofluid based flat-plate solar collector. *Appl. Therm. Eng.* **2016**, *98*, 1116–1129. [CrossRef]
91. Ahmadi, A.; Ganji, D.D.; Jafarkazemi, F. Analysis of utilizing Graphene nanoplatelets to enhance thermal performance of flat plate solar collectors. *Energy Convers. Manag.* **2016**, *126*, 1–11. [CrossRef]
92. Jeon, J.; Park, S.; Lee, B.J. Analysis on the performance of a flat-plate volumetric solar collector using blended plasmonic nanofluid. *Sol. Energy* **2016**, *132*, 247–256. [CrossRef]
93. Verma, S.K.; Tiwari, A.K.; Chauhan, D.S. Experimental evaluation of flat plate solar collector using nanofluids. *Energy Convers. Manag.* **2017**, *134*, 103–115. [CrossRef]
94. Genc, A.M.; Ezan, M.A.; Alpaslan, T. Thermal performance of a nanofluid-based flat plate solar collector: A transient numerical study. *Appl. Therm. Eng.* **2018**, *130*, 395–407. [CrossRef]
95. Sharma, N.; Diaz, G. Performance model of a novel evacuated-tube solar collector based on minichannels. *Sol. Energy* **2011**, *85*, 881–890. [CrossRef]
96. Khamis Mansour, M. Thermal analysis of novel minichannel-based solar flat-plate collector. *Energy* **2013**, *60*, 333–343. [CrossRef]
97. Deng, Y.; Zhao, Y.; Wang, W.; Quan, Z.; Wang, L.; Yu, D. Experimental investigation of performance for the novel flat plate solar collector with micro-channel heat pipe array (MHPA-FPC). *Appl. Therm. Eng.* **2013**, *54*, 440–449. [CrossRef]
98. Oyinlola, M.A.; Shire, G.S.F.; Moss, R.W. Thermal analysis of a solar collector absorber plate with microchannels. *Exp. Therm. Fluid Sci.* **2014**, *67*, 102–109. [CrossRef]
99. Oyinlola, M.A.; Shire, G.S.F.; Moss, R.W. Investigating the effects of geometry in solar thermal absorber plates with micro-channels. *Int. J. Heat Mass Transf.* **2015**, *90*, 552–560. [CrossRef]
100. Azad, E. Theoretical and experimental investigation of heat pipe solar collector. *Exp. Therm. Fluid Sci.* **2008**, *32*, 1666–1672. [CrossRef]
101. Azad, E. Assessment of three types of heat pipe solar collectors. *Renew. Sustain. Energy Rev.* **2012**, *16*, 2833–2838. [CrossRef]
102. Wei, L.; Yuan, D.; Tang, D.; Wu, B. A study on a flat-plate type of solar heat collector with an integrated heat pipe. *Sol. Energy* **2013**, *97*, 19–25. [CrossRef]
103. Zhu, T.; Diao, Y.; Zhao, Y.; Ma, C. Performance Evaluation of a Novel Flat-Plate Solar Air Collector with Micro-Heat Pipe Arrays (MHPA). *Elsevier Appl. Therm. Eng.* **2017**, *118*, 1–16. [CrossRef]
104. Zhu, T.; Diao, Y.; Zhao, Y.; Deng, Y. Experimental study on the thermal performance and pressure drop of a solar air collector based on flat micro-heat pipe arrays. *Energy Convers. Manag.* **2015**, *94*, 447–457. [CrossRef]
105. Ersoz, M.A. Effects of different working fluid use on the energy and exergy performance for evacuated tube solar collector with thermosyphon heat pipe. *Renew. Energy* **2016**, *96*, 244–256. [CrossRef]
106. Zhang, D.; Tao, H.; Wang, M.; Sun, Z.; Jiang, C. Numerical simulation investigation on thermal performance of heat pipe flat-plate solar collector. *Appl. Therm. Eng.* **2017**, *118*, 113–126. [CrossRef]
107. Wang, T.; Diao, Y.; Zhao, Y.; Liang, L.; Wang, Z.; Chen, C. A comparative experimental investigation on thermal performance for two types of vacuum tube solar air collectors based on flat micro-heat pipe arrays (FMHPA). *Sol. Energy* **2020**, *201*, 508–522. [CrossRef]
108. Eaton, C.B.; Blum, H.A. The use of moderate vacuum environments as a means of increasing the collection efficiencies and operating temperatures of flat-plate solar collectors. *Sol. Energy* **1975**, *17*, 151–158. [CrossRef]
109. Benz, N.; Beikircher, T. High efficiency evacuated flat-plate solar collector for process steam production. *Sol. Energy* **1999**, *65*, 111–118. [CrossRef]
110. Arya, F.; Hyde, T.; Henshall, P.; Eames, P.; Moss, R.; Shire, S. Current Developments in Flat-Plate Vacuum Solar Thermal Collectors. *Int. J. Energy Power Eng.* **2016**, *10*, 688–692.
111. Arya, F.; Hyde, T.; Henshall, P.; Eames, P.; Moss, R.; Shire, S. Fabrication and Characterisation of Slim Flat Vacuum Panels Suitable for Solar Applications. In Proceedings of the EuroSun: International Conference on Solar Energy and Buildings, Aix-Les-Bains, France, 16–19 September 2014; 16 September 2014. [CrossRef]
112. Buttinger, F.; Beikircher, T.; Pro, M.; Scho, W. Development of a new flat stationary evacuated CPC-collector for process heat applications. *Sol. Energy* **2010**, *84*, 1166–1174. [CrossRef]
113. Henshall, P.; Moss, R.; Arya, F.; Eames, P.C.; Shire, S.; Hyde, T. An evacuated enclosure design for solar thermal energy applications. *Gd. Renew. Energy* **2014**, *2014*, 2–5.
114. Arya, F.; Hyde, T.; Henshall, P.; Eames, P.; Moss, R.; Shire, S.; Uhomoibhi, J. Fabrication analysis of flat vacuum enclosures for solar collectors sealed with Cerasolzer 217. *Sol. Energy* **2021**, *220*, 635–649. [CrossRef]
115. Available online: tvpSolar.com (accessed on 26 January 2021).

116. Available online: http://digicollection.org/eebea/documents/s20413en/s20413en.pdf (accessed on 20 March 2021).
117. Henshall, P.; Eames, P.; Arya, F.; Hyde, T.; Moss, R.; Shire, S. Constant temperature induced stresses in evacuated enclosures for high performance flat plate solar thermal collectors. *Sol. Energy* **2016**, *127*, 250–261. [CrossRef]